Journal of Power Sources 187 (2009) 247–252

Contents lists available at ScienceDirect

Journal of Power Sources

journal homepage: www.elsevier.com/locate/jpowsour

Mechanochemical synthesis of $NaMF_3$ (M = Fe, Mn, Ni) and their electrochemical properties as positive electrode materials for sodium batteries

Irina D. Gocheva[a], Manabu Nishijima[a], Takayuki Doi[b], Shigeto Okada[b,*], Jun-ichi Yamaki[b], Tetsuaki Nishida[c]

[a] Interdisciplinary Graduate School of Engineering and Material Sciences, Kyushu University, 6-1 Kasuga Koen, Kasuga-shi 816-8580, Japan
[b] Institute of Materials Chemistry and Engineering, Kyushu University, 6-1 Kasuga Koen, Kasuga-shi 816-8580, Japan
[c] School of Humanity-Oriented Science and Engineering, Kinki University Kayanomori, Iizuka 820-8555, Japan

ARTICLE INFO

Article history:
Received 31 August 2008
Received in revised form 24 October 2008
Accepted 28 October 2008
Available online 6 November 2008

Keywords:
Mechanochemical sodiation
Transition metal fluorides

ABSTRACT

Mechanical treatment was used as a nonconventional solid-state process for large-scale preparation of fluoride materials as an alternative to the hazardous high-pressure fluorination route. Sodium fluoroperovskites of Fe, Mn, and Ni were achieved by mechanical grinding of NaF and binary metal fluorides for different periods of time under Ar. The obtained monophases were characterized by XRD measurements, AAS, ICP-OES, and IC. The electrochemical performance of the achieved materials was tested in a Na half-cell under different operating conditions. It was revealed that mechanochemically inserted sodium is electrochemically active for the $NaFeF_3$ positive electrode composition. In this pilot study, $NaFeF_3$ showed an initial discharge capacity of 130 mA h g^{-1} at 0.2 mA cm^{-2}.

1. Introduction

The most studied cathode materials for lithium batteries are crystalline cobalt-, manganese- and nickel-based oxides. Li-ion batteries should fulfill a variety of safety, environmental, price, and energy density demands. In this context, polyanion-type cathode materials with a cheap and environmentally friendly transition element (i.e. Mn and Fe), seem to be a good choice [1]. Currently, some new fluoride-based cathode materials have provoked attention in attempts to overcome the theoretical capacity limit of polyanionic cathodes [2–4]. Although the high output voltages due to the high electronegativity of fluorine are attractive and compatible with many 3 V needs, the performance first reported for FeF_3 was not significant [5]. However, the high reversible capacity beyond 200 mA h g^{-1}, larger than that of $LiFePO_4$, was recently achieved in FeF_3/C nano-composites electrodes [6,7].

Nevertheless, metal fluorides have not been known as positive electrode materials until now because of their difficulties of synthesis, for example in high-pressure fluorination with F_2 gas [8]. Other synthesis routes reported are solid-state reactions under inert conditions and high temperatures [9], thermal degradation of functional fluorides [10], complex formation reactions by precipitation with HF acid [11], and hydrothermal synthesis of complex fluorides [12], but they require a complicated apparatus and strict control of extreme operating conditions.

Recently, a mechanically induced solid-state chemical reaction was used as an alternative synthesis route for functional fluorides such as $AZnF_3$ compounds (A = K, Na, NH_4) with a perovskite structure [13], ARF_4 (A = Li, Na, K; R = rare-earth elements), nanosized complex fluorides [14], and KMF_3 (M = Mg, Ca, Mn, Fe, Co, Ni, Zn) cubic potassium fluoroperovskites [15], cryolite Na_3AlF_6 and chiolite $Na_5Al_3F_{14}$ [16]. But the present knowledge concerning mechanochemical activation of solid fluorides is still insufficient. Fluorides are basically unstable with moisture, which leads to decomposition. They hurt the surfaces of chemical reactors and containers and stick to them. In addition, the high-ionic and low-hardness character of fluorides complicates their mechanochemical development compared to the oxides.

The purpose of this paper is to provide information regarding the mechanochemical sodiation of some transition metal fluorides M = Fe, Mn, Ni, as well to reveal their possible properties as cathode active materials in rechargeable batteries. In fact, sodium-ion batteries could be an attractive substitute for their lithium-ion counterparts, and may bring some advantages such as low materials costs and environmental impact, even if the standard electrode potential of Na (−2.71 V vs. SHE) is not low as that of Li (−3.05 V vs. SHE) and the ionic volume of sodium is almost twice that of lithium ion. Sodium-based systems suffer from lack of suitable cathode and anode active materials. However, that situation has been improving gradually. It was recently found that some carbon materials exhibit

* Corresponding author. Tel.: +81 92 583 7841; fax: +81 92 583 7841.
E-mail address: s-okada@cm.kyushu-u.ac.jp (S. Okada).

0378-7753/$ – see front matter © 2008 Elsevier B.V. All rights reserved.
doi:10.1016/j.jpowsour.2008.10.110

high reversible capacity for Na-ion insertion up to 350 mA h g^{-1} [17,18]. Our group also confirmed that FeF_3 and VF_3 cathodes have suitable electrochemical performance not only with Li but also vs. Na metal anode [19]. These new findings encourage us to investigate $NaMF_3$ ternary metal fluorides as cathode candidates for sodium-ion batteries with carbonaceous anodes.

2. Experimental

2.1. Preparation

An equimolar mixture of sodium fluoride (NaF) and one of transition metal fluoride (MF_2) (M = Mn, Fe, Ni) 99% purity provided by and SOEKAWA Chemicals Ltd., Japan were ground by using a planetary type ball mill Pulverisette-7 Premium line (FRITSCH GmbH, Germany) under the following conditions: sample weight, 3 g; grinding media: 250 balls with a diameter of 4 mm; milling media and chamber material: zirconium oxide; mill speed: 750 rpm, for different dry milling times in Ar atmosphere. Fixed milling regimes guaranteed the reproducibility of repeated experiments. All air- and moisture-sensitive materials were handled in an Ar-filled dry box to avoid possible fluorine losses.

2.2. Characterization

The reaction products were estimated by XRD powder diffraction (Rigaku RINT2100HLR/PC) using Cu Kα radiation from 2θ = 10–80° at a 0.03° s^{-1} scan rate. The morphology and particle size distribution of ground samples were observed by FE-SEM (JEOL JSM-340F) and a dynamic light scattering analyzer (Horiba LA-300). Thermal stability of the obtained materials was investigated by TG-DSC (Rigaku Thermo Plus TG8210) with a heating rate of 5 °C min^{-1} up to 500 °C in an Ar atmosphere. XPS measurements were accomplished with a JPS-9000 (JEOL Ltd.). Mössbauer spectroscopy was applied to consider changes in the iron oxidation state. A constant acceleration method was performed using the Mössbauer spectrometer (Laboratory Equipment Corp.). As the Mössbauer source and the reference for the isomer shift we used 370 MBq of ^{57}Co (Pd) and α-Fe foil enriched with ^{57}Fe. Chemical analysis has been accomplished by AAS (Hitachi Z-2300), ICP-OES (SII Nano Technology Inc. SPS 4000), and ion chromatography (DIONEX DX-500) to confirm the element composition of the obtained fluoroperovskites.

Electrochemical evaluation of the synthesized materials was carried out in a coin-type cell 2032 with Na metal as a negative electrode in 1 M $NaClO_4$/PC electrolyte composition with a polypropylene separator Celgard 3501. The positive electrodes with loadings of approximately 30 mg were composed of 70 wt.% active material, 25 wt.% acetylene black, and 5 wt.% PTFE as binder. An electrode diameter of 10 mm was used throughout. Cycling tests were performed using an automatic galvanostatic charge–discharge unit (Nagano BTS-2004) at various current densities between 1.5 and 4.0 V at an ambient temperature of 25 °C.

3. Results and discussion

Sodium iron fluoroperovskite could be obtained by triggering a chemical reaction through the use of mechanical forces instead of thermochemical activation, as shown on the XRD pattern (Fig. 1). In all diffractograms, which suggested different milling times of 60, 90, and 130 min, respectively, no peaks of starting materials were observed. The material is consistent with corresponding ICDD No. 43-0705 and is identified as orthorhombic perovskite of space group *P*nma. Apparently, increasing the grinding period leads to fast amorphization of fluoroperovskite materials with weaker

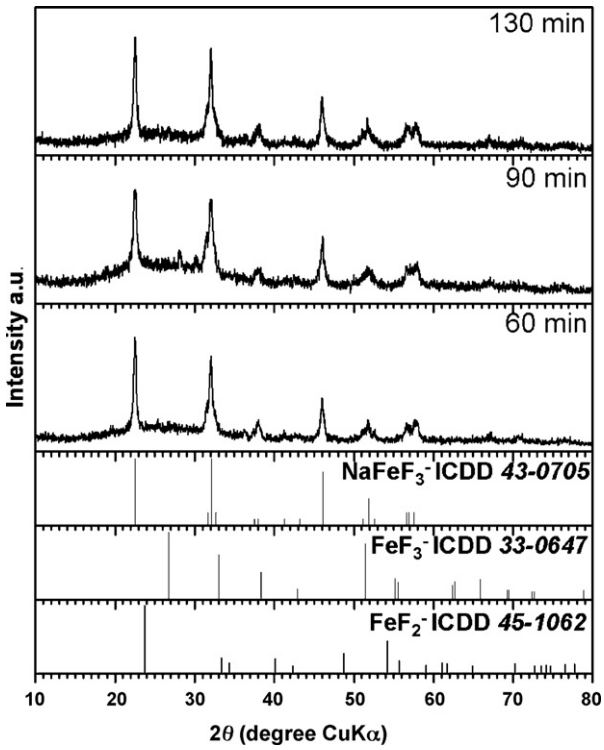

Fig. 1. XRD pattern for mechanochemically obtained $NaFeF_3$ with dependence on the milling time.

peak intensity, but generally there are no visible differences in XRD patterns of the materials grounded for more than 60 min, which implies that structures could be sustained against prolonged milling. The position of XRD reflections in patterns of the obtained materials displays that ternary fluorides can be synthesized by mechanical sodiation with no detectable impurities through following reaction:

$$NaF + MF_2 \rightarrow NaMF_3$$

Lattice parameters calculated on the basis of XRD data optimized by least square refinement (Table 1) show slightly larger values for this research compared to those cited in ICDD, because with the milling process some distortions are induced in the structure. Chemical analysis of the powder compound obtained throughout mechanical mixing of equimolar amounts of NaF and FeF_2 gave the following results for chemical composition: Na, 15.6 wt.%; Fe, 37.5 wt.%; F, 40.1 wt.% (theoretically Na, 16.9 wt.%; Fe, 41.1 wt.%; F, 41.9 wt.%).

Morphological observation of the dry ball milled materials (Fig. 2) proves that synthesized $NaFeF_3$ homogeneous powder consisting of primary particles of nanometer range. However, they tend to agglomerates with an average distribution ca. 6 μm. This result is attributed to the dry ball milling procedure applied. The

Table 1
Calculated lattice parameters for mechanochemically synthesized $NaFeF_3$ with dependence on the milling time.

Compound	Lattice parameters (Å)			
	a	*b*	*c*	*V* (Å^3)
$NaFeF_3$				
Synthesized for 60 min	5.45(3)	5.71(6)	8.0(2)	248.9
Synthesized for 90 min	5.43(2)	5.70(5)	8.0(2)	247.6
Synthesized for 130 min	5.56(6)	5.68(8)	7.8(12)	246.3
ICDD-43-0705	5.483	5.657	7.875	244.3

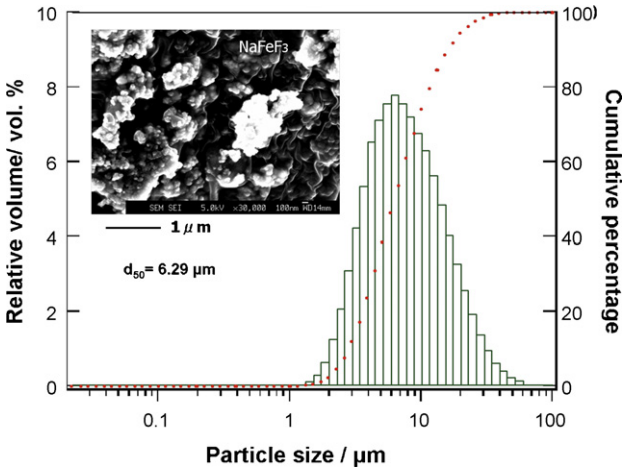

Fig. 2. FE-SEM image and PSD for $NaFeF_3$.

thermal stability of the powdered $NaFeF_3$ was studied by TG-DSC analysis in Ar, where any exothermal peak caused by phase transition or significant mass loss was not observed up to 500 °C in the system.

XPS measurements have been undertaken in order to further examine the composition and bond types of powdered $NaFeF_3$ obtained by mechanochemical grinding (Fig. 3). Owing to the near ionic radius of fluorine and oxygen, the latter could enter the fluoride crystal lattice, replacing fluorine in the structure. Therefore, when the oxygen content in fluoride products is high, the electron binding energy of the atom inner shell would change with changes in the chemical environment, and as a result the symmetry of the XPS peaks of each element will change remarkably due to the M–O and F–O bonds. It can be seen from the tabulated results for present study that the F(ls) binding energy of 685.3 eV is in good agreement with the corresponding FeF_2 and NaF values of starting compounds. The peak shape of F(1s) envelope also indicates that the F–O bond

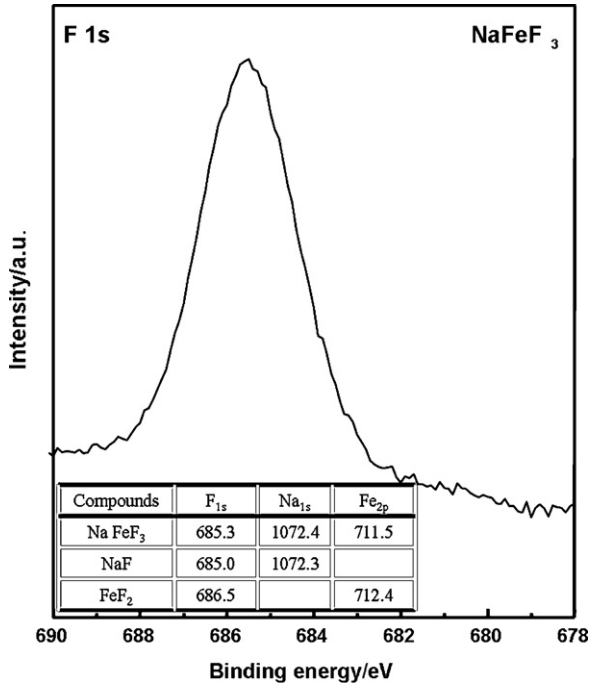

Compounds	F_{1s}	Na_{1s}	Fe_{2p}
$Na FeF_3$	685.3	1072.4	711.5
NaF	685.0	1072.3	
FeF_2	686.5		712.4

Fig. 3. F 1s XPS spectra and tabulated data of binding energies (eV) for powder $NaFeF_3$ obtained by mechanical grinding under Ar.

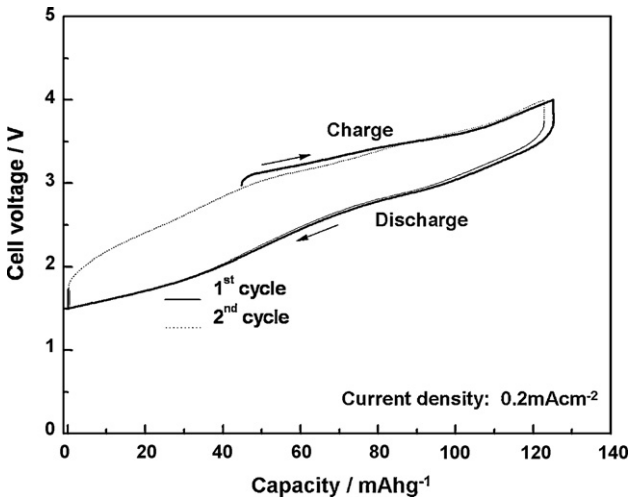

Fig. 4. First and second charge/discharge profiles of $NaFeF_3$ synthesized after 130 min ball milling at 750 rpm in Ar vs. Na metal anode. The voltage range was suggested to be 1.5–4.0 V.

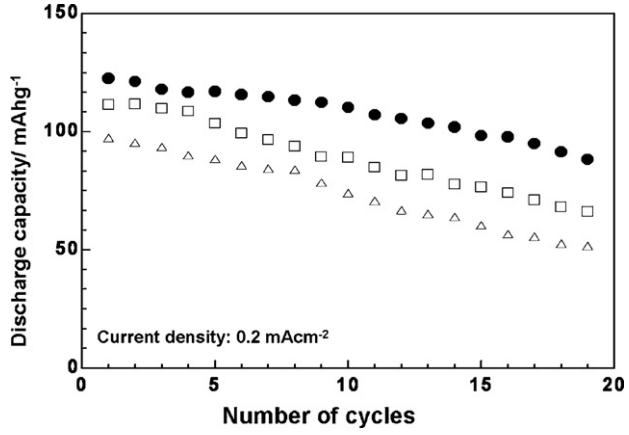

Fig. 5. Cycle performance of $NaFeF_3$ vs. Na metal anode as a function of the milling time (△: samples achieved by mechanical milling for 60 min; □: samples milled for 90 min; ●: samples milled for 130 min).

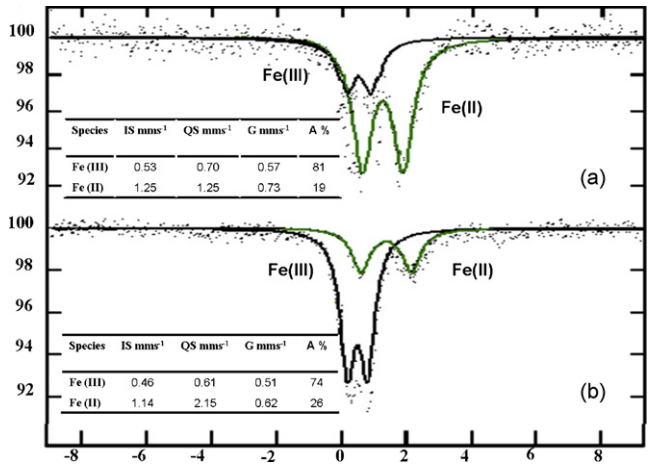

Fig. 6. ^{57}Fe Mössbauer spectra of (a) mechanical sodiated and (b) fully charged $NaFeF_3$/Na pellets.

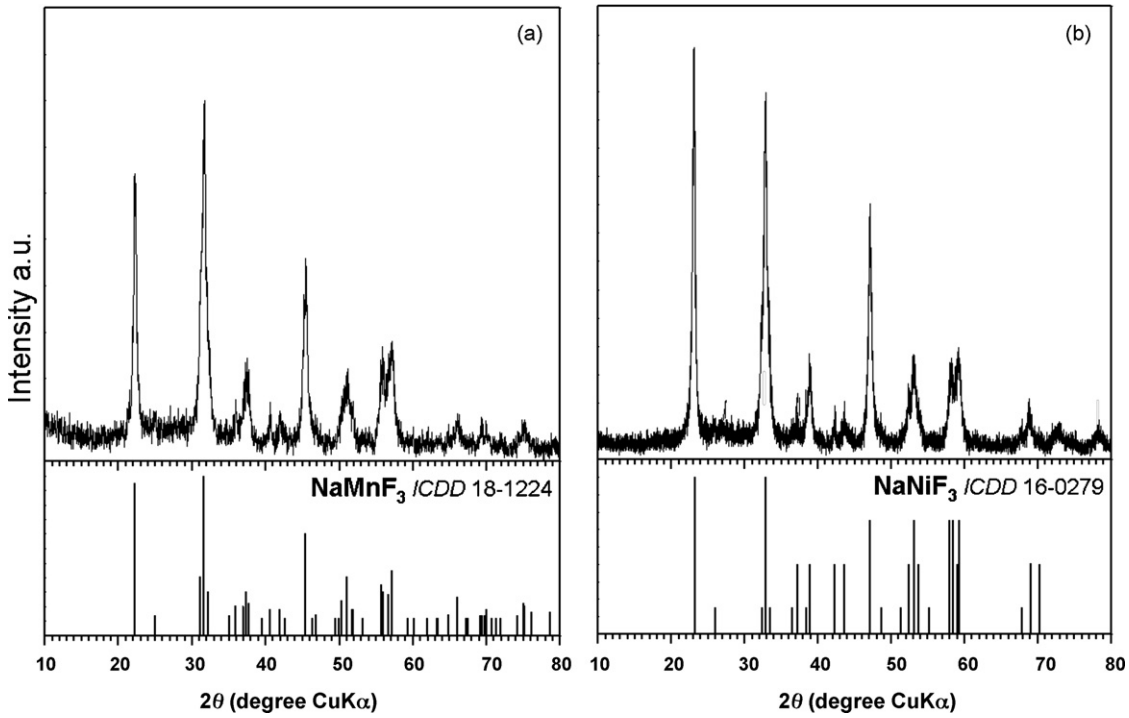

Fig. 7. XRD pattern for (a) mechanochemically obtained $NaMnF_3$ and (b) $NaNiF_3$.

is not formed in $NaFeF_3$ and that the oxygen content is practically negligible for materials achieved by mechanochemical synthesis.

The results for the charge/discharge profiles of $NaFeF_3$ cathode vs. Na negative electrode are shown in Fig. 4. A representative cell was cycled between 1.5 and 4.0 V with a current of 0.2 mA cm^{-2}. The first discharge capacity of the $NaFeF_3$/Na cell was 128 mA h g^{-1} with an average cell voltage of 2.7 V. We found that by enhancing the strength of the impact for periods of grinding of 130 min, the electrochemical performance of the obtained material was improved as a consequence of reduced particle size, as shown in Fig. 5. It was noted that the first charge capacity was approximately 50 mA h g^{-1} smaller than the first discharge capacity (128 mA h g^{-1}). This difference could be explained by the partial sodiation of iron fluoride matrix compensated by Na metal anode for the next cycle. The obtained discharge capacity was approximately 65% of the theoretical capacity. This is owing to the high polarization caused by the poor kinetics of the large sodium ion. The irreversibility observed could be due to the slight dissolution of the ionic fluoride cathode in electrolyte. This would be avoided through careful choice of the electrolyte composition and optimization of the carbon-coating treatment on the cathode surface in future experiments.

^{57}Fe Mössbauer spectra of mechanical sodiated and fully charged Na_xFeF_3 samples at RT are presented in Fig. 6. Both spectra consist of two symmetric doublets. It shows that the matrixes of the mechanically sodiated sample had high-spin Fe(II) and Fe(III) with 81:19 atom%, respectively (Fig. 6a). The presence of

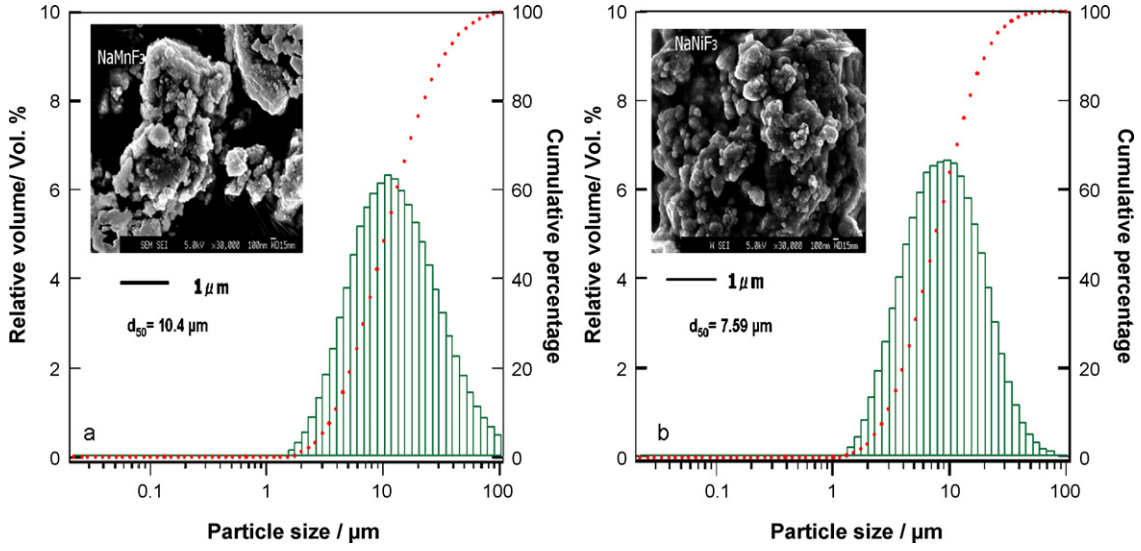

Fig. 8. FE-SEM image and PSD for (a) $NaMnF_3$ and (b) $NaNiF_3$.

19% Fe(III) in the initial condition could be explained as a result of the mechanical-electron effect induced by the extended milling; therefore, mechanochemical sodiation was incomplete, which is consistent with the discrepancy between the initial charge and discharge capacity, as shown in Fig. 4. In the fully charged state (Fig. 6b), the strong intensity of the small symmetric doublet with an isomer shift of $0.46 \pm 0.01\ mm\ s^{-1}$ indicates that Fe(II) is oxidized to Fe(III) by sodium extraction during charging. However, the remaining signal of Fe(II) reflects the insufficient charge/discharge process of the sodium cells examined by our laboratory.

XRD patterns of mechanochemically achieved $NaMnF_3$ and $NaNiF_3$ are shown in Fig. 7. The structure of $NaMnF_3$ at room temperature is orthorhombic with a slight distortion from ideal symmetry caused by the tilting of MnF_6 octahedrons [20]. Chemical analysis of the powder compounds yielded the following: Na, 16.5 wt.%; Mn, 39.5 wt.%; F, 43.2 wt.% (calculated Na, 17.0 wt.%; Mn, 40.7 wt.%; F, 42.2 wt.%) and Na, 16.9 wt.%; Ni, 39.4 wt.%; F, 42.1 wt.% (calculated Na, 16.8 wt.%; Ni, 42.3 wt.%; F, 41.1 wt.%) which are in good agreement for the compounds obtained by mechanochemical grinding.

The SEM observations of $NaMnF_3$ and $NaNiF_3$ are shown in Fig. 8. As the photographs indicate, the crystallites have regular morphology, with an average particle size distribution of 10.4 μm for $NaMnF_3$ and 7.59 μm for $NaNiF_3$. The electrochemical performance of the obtained materials studied following the above listed protocol was insufficient in practical cells. The results regarding cycle performance and the practical discharge capacity of both $NaMnF_3$ and $NaNiF_3$ are shown in Fig. 9. Poor electronic conductivity due to the large band gap induced by the Mn–F and Ni–F bonds appears to be a possible reason for the low capacity of such materials. On the other hand, assuming the logic that according to the standard electrode potential difference vs. Li/Li^+ for $Fe^{3+}/Fe^{2+} = 3.49$ V while $Mn^{3+}/Mn^{2+} = 4.2$ V, we expected that the Mn-containing compound (Fig. 10a) would have a higher mean cell voltage than that of Fe–F matrix also in sodium cell. In addition, cutoff voltage restricted up to 4 V to prevent electrolyte decomposition, limited charge of $NaMnF_3$/Na and $NaNiF_3$/Na cells this might explain why we do not obtain a large capacity for those materials. We believe that a bet-

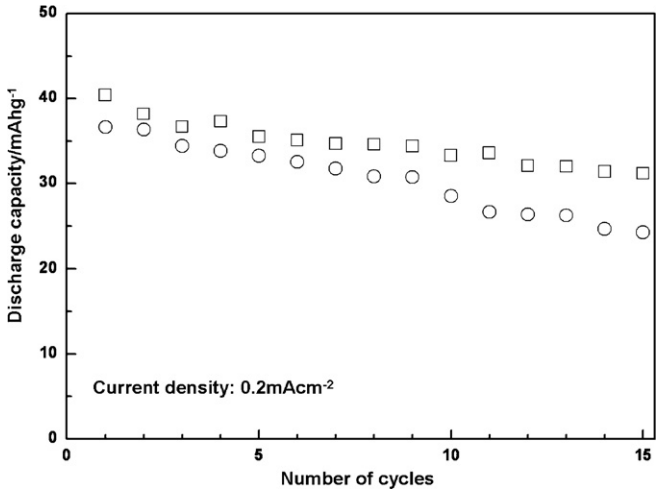

Fig. 9. Cycle performance of $NaMnF_3$ and $NaNiF_3$ synthesized after 130 min ball milling at 750 rpm in Ar vs. Na metal anode (□: $NaMnF_3$: ○: $NaNiF_3$).

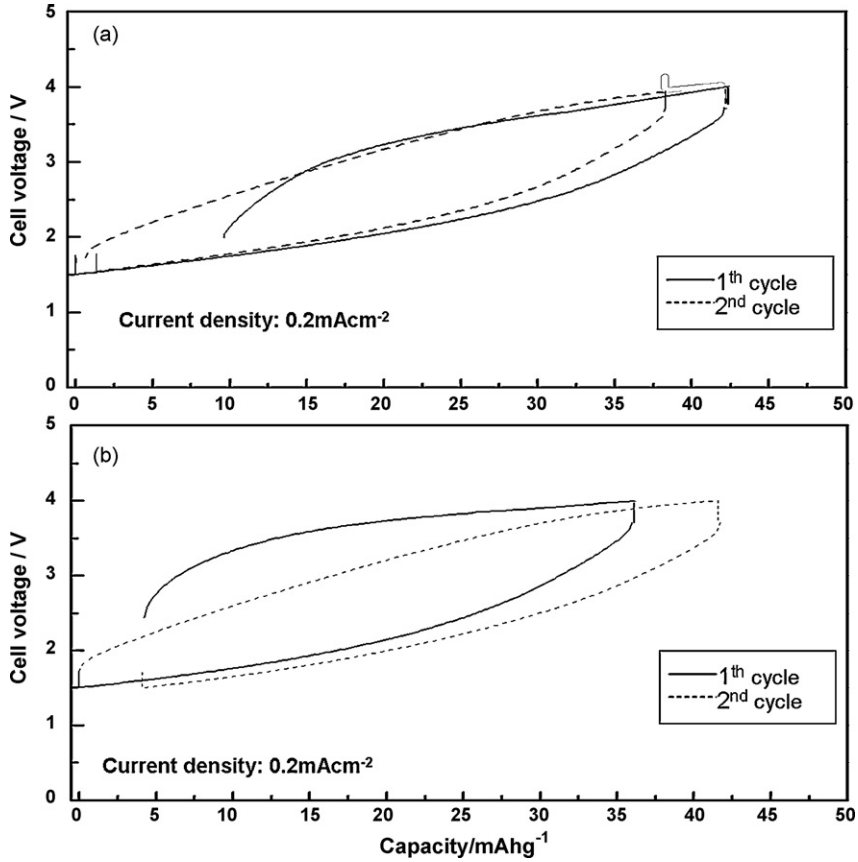

Fig. 10. First and second charge/discharge profiles of (a) $NaMnF_3$ and (b) $NaNiF_3$ achieved after 130 min ball milling at 750 rpm in Ar vs. Na metal anode.

ter oxidation-resistant electrolyte up to 5 V will improve the true electrochemical performance of $NaMnF_3$ and $NaNiF_3$ which might be better than that of $NaFeF_3$.

4. Conclusions

Synthesis of perovskite type sodium metal fluorides, $NaMF_3$ (M = Fe, Mn, Ni) was attempted for the first time mechanochemically by grinding mixtures of MF_2 and NaF in Ar at low temperature. The grinding allows us to synthesize these compounds at room temperature and to investigate the crystallinity of compounds in relation to the grinding process. The electrochemical properties of prepared materials revealed that $NaFeF_3$ milled for 130 min exhibits a mean discharge voltage of 2.7 V and a reversible capacity of 120 mA h g^{-1} in a Na/Na^+ cell. Although it displayed relatively poor rate capabilities in this initial stage of research, $NaFeF_3$ does have promising characteristics. Certainly, such sodium compensation, which has been noted as important to cell performance, cannot be expected in a practical ion cell using a carbon anode, but it does provide evidence that mechanochemically inserted sodium is electrochemically active and intrinsically reversible. As for the other two compounds under study, $NaMnF_3$ and $NaNiF_3$, further work is needed, particularly for the improvement of electrochemical performance. It is noteworthy that a large octahedral A-site for sodium in the MF_3 perovskite framework could be used as new cathode/anode materials for sodium-ion batteries. The fluoroperovskites are a new cathode/anode candidate, their properties and prospective uses in practical battery are still in an undeveloped and unexcavated state.

Acknowledgement

The present work was financially supported by the Li-EAD project of the New Energy and Industrial Technology Development Organization, Japan.

References

[1] A.K. Padhi, K.S. Nanjundaswamy, C. Masquelier, S. Okada, J.B. Goodenough, J. Electrochem. Soc. 144 (1997) 1609–1613.
[2] Y. Makimura, A. Rougier, J.M. Tarascon, Appl. Surf. Sci. 252 (2006) 4587–4592.
[3] H. Li, P. Balaya, J. Maier, Adv. Mater. 15 (9) (2003) 737–739.
[4] M. Bervas, et al., J. Electrochem. Soc. 153 (4) (2006) A799–A808.
[5] H. Arai, S. Okada, Y. Sakurai, J. Yamaki, J. Power Sources 68 (1997) 716–721.
[6] F. Badway, N. Pereira, F. Cosandey, G.G. Amatucci, J. Electrochem. Soc. 150 (9) (2003) A1209–A1218.
[7] F. Badway, F. Cosandey, N. Pereira, G.G. Amatucci, J. Electrochem. Soc. 150 (10) (2003) A1318–A1327.
[8] R. Bougon, J. Ehretsmann, J. Portier, A. Tressaud, in: P. Hagenmuller (Ed.), Preparative Methods in Solid State Chemistry, Academic Press, New York, 1972, pp. 401–433.
[9] G. Brenner, R. Hoppe, J. Fluorine Chem. 46 (1990) 283–295.
[10] A. Epstein, J. Markovsky, M. Melamud, H. Shaked, Phys. Rev. 174 (2) (1968) 174–175.
[11] J.L. Fourquet, Y. Calage, U. Bentrup, J. Solid State Chem. 108 (1994) 189–192.
[12] H. Li, Z. Jia, C. Shi, Chem. Lett. 29 (9) (2000) 1106–1107.
[13] J. Lee, Q. Zhang, F. Saito, Chem. Lett. 30 (7) (2001) 700–701.
[14] J. Lu, Q. Zhang, F. Saito, Chem. Lett. 31 (12) (2002) 1176–1177.
[15] J. Lee, H. Shin, J. Lee, H. Chung, Q. Zhang, F. Saito, Mater. Trans. 44 (2003) 1457–1460.
[16] G. Scholz, O. Korup, Solid State Sci. 8 (2006) 678–684.
[17] D.A. Stevens, J.R. Dahn, J. Electrochem. Soc. 147 (2000) 1271–1273.
[18] D.A. Stevens, J.R. Dahn, J. Electrochem. Soc. 148 (2001) A803–A811.
[19] M. Nishijima, I.D. Gocheva, S. Okada, J. Yamaki, J. Power Sources (submitted).
[20] A. Ratuszna, K. Majewska, Acta Cryst. C45 (1989) 548–551.